Rev.Adv.Mater.Sci. 14(2007) 49-56

EPR, OPTICAL AND DIELECTRIC PROPERTIES OF $Sr_{0.33}Ba_{0.67}Nb_2O_6$ AND $Sr_{0.58}Ba_{0.42}Nb_2O_6$ SINGLE CRYSTALS PURE AND DOPED WITH CHROMIUM AND YTTERBIUM

S.M. Kaczmarek[1], M. Berkowski[2], K. Repow[1], M. Orłowski[1], A. Worsztynowicz[1] and M. Włodarski[3]

1 - Institute of Physics, Szczecin University of Technology, 48 Al. Piastów, 70-310 Szczecin, Poland
2 - Institute of Physics Polish Academy of Sciences, 32/46 Al. Lotników, 02-668 Warsaw, Poland
3 – Institute of Optoelectronics, Military University of Technology, 2 Kaliski, 00-908 Warsaw, Poland

Received: December 08, 2006

Abstract. Two types of SBN crystals were grown and analyzed for their spectroscopic and dielectric properties: $Sr_{0.33}Ba_{0.67}Nb_2O_6$: Cr and $Sr_{0.58}Ba_{0.42}Nb_2O_6$: Cr, Yb. The absorption and EPR spectra show the presence of Cr^{3+} at interstitial ions beside the ions substituted for Nb^{5+}. Unexpectedly, Yb^{3+} has not entered to the $Sr_{0.58}Ba_{0.42}Nb_2O_6$: Cr crystal at Nb^{5+} octahedral sites. The crystals differ significantly each other especially for their dielectric properties mainly due to stoichiometry. The former crystal exhibits ferroelectric phase transition at about 378K, while the latter at 340K. We have found spontaneous polarization being equal to 2,44 $\mu C/cm^2$ (SBN:33:Cr) and to 1 $\mu C/cm^2$ (SBN:58:Cr:Yb).

1. INTRODUCTION

$Sr_xBa_{1-x}Nb_2O_6$ (SBN) is a considerably more efficient second harmonic generator than previously known materials and is also stable to focused laser radiation at 0.488 mm. It is attractive for various applications, particularly for optical storage and light wave amplification. SBN is reported to have an unusually large transverse electro-optic effect at room temperature. Doping of SBN crystals with rare-earth impurities strongly lowers the ferroelectric phase transition T_c which results in a significant enhancement of the dielectric permittivity and electrooptic coefficients, and in a simultaneous decrease of the coercive field E_c [1]. Photorefractive properties of SBN crystals (x=0.61 congruent) can be enhanced more by doping with cerium and chromium [2]. Cr doped $Sr_{0.6}Ba_{0.4}Nb_2O_6$ (SBN:60:Cr) crystals have previously been observed to exhibit increased photorefractive gain as the crystal temperature is lowered below room temperature and away from its ferroelectric phase transition near 345K [3]. SBN crystal is also very nice relaxor due to its wide phase transition from a ferro- to a paraelectric phase with no strong structural changes around room temperatures [4]. Polarization still exists at temperatures much larger then T_c. This behavior originates from the dynamics of nano-domains (polar clusters). The properties of the domains and, thus, diffuseness of the phase transition are controlled by composition and impurities. In this paper we report spectral and dielec-

Corresponding author: S.M. Kaczmarek, e-mail: skaczmarek@ps.pl

tric properties of Cr^{3+} and Cr^{3+}, Yb^{3+} doped SBN single crystal obtained in the Institute of Physics SUT, Szczecin.

2. EXPERIMENTAL

$Sr_{0.33}Ba_{0.67}Nb_2O_6$:Cr (SBN:33:Cr) and $Sr_{0.58}Ba_{0.42}Nb_2O_6$:Cr, Yb (SBN:58:Cr:Yb) single crystals were obtained using Czochralski method within MSR4. Iridium crucible of 40 mm in diameter was used heated by applying the induction furnace. Oxides of 4N and 5N purity were used as starting materials. Before weighting the oxides were heated for 4 hours at temperature of 1000 °C. Stoichiometric mixture of oxides was used as a starting composition, without previous synthesis. The growth rate was 1.5 mm/h and the rotation rate of the crucible was 20 rpm. Pure nitrogen was used as an inert atmosphere with oxygen partial pressure, measured in output gas, lower than 500 ppm. We have observed segregation of Sr content with respect to Ba during the growth.

The obtained crystals revealed spiral growth and were not transparent due to nitrogen atmosphere during the growth, so they had to be annealed in the air at 1273K for 3h. Because of the oxidizing annealing, the samples had to be irradiated with γ-quanta to show Cr^{3+} photoluminescence (PL).

The structure of these crystals was investigated by X-ray powder diffraction (XRD) method. The XRD pattern of the two crystals is presented in Fig. 1. It was found that both crystals had tetragonal structure with lattice cell parameters: SBN:33:Cr (0.02 mol.%) - a=12.482641 (0.000632) Å, c=3.981882 (0.000443) Å, V=620.44 Å^3, Z=5 in agreement with previously published: a= 12.496(3) Å, c=3.973(5) Å, V= 620.38 Å^3 [5]; SBN:58:Cr:Yb (0.02 mol.%, 0.5 mol.%) - a=12.462678 (0.000465) Å, c=3.935047 (0.000187) Å, V=611.18 Å^3 in agreement with previously published: a=12.4652 Å, c=3.9521 Å, V= 614.08 Å^3 [6], and space group Pb4m [7].

To perform the spectroscopic measurements, plates were cut from bulk crystal and polished with the surfaces perpendicular to the c-axis, 1 mm in thickness. The samples were examined for the transmission before and followed by γ-irradiation with a dose of $1.2 \cdot 10^5$ Gy. Additional absorption was calculated according to formula:

$$\Delta K(\lambda) = 1/d \cdot \ln(T_1/T_2), \quad (1)$$

where T_1 and T_2 are transmissions of the sample measured before and after γ-irradiation, respectively, d – sample thickness, K – absorption and λ - wavelength. Transmission measurements were made at room temperature using Lambda-900 of Perkin-Elmer spectrophotometer in the range of 190-3200 nm, while photoluminescence (PL) measurements using a SS-900 Edinburgh Inc. spectrophotometer in the Institute of Optoelectronics, MUT, Poland.

Electron Paramagnetic Resonance (EPR) spectra were registered using a standard X-band Bruker

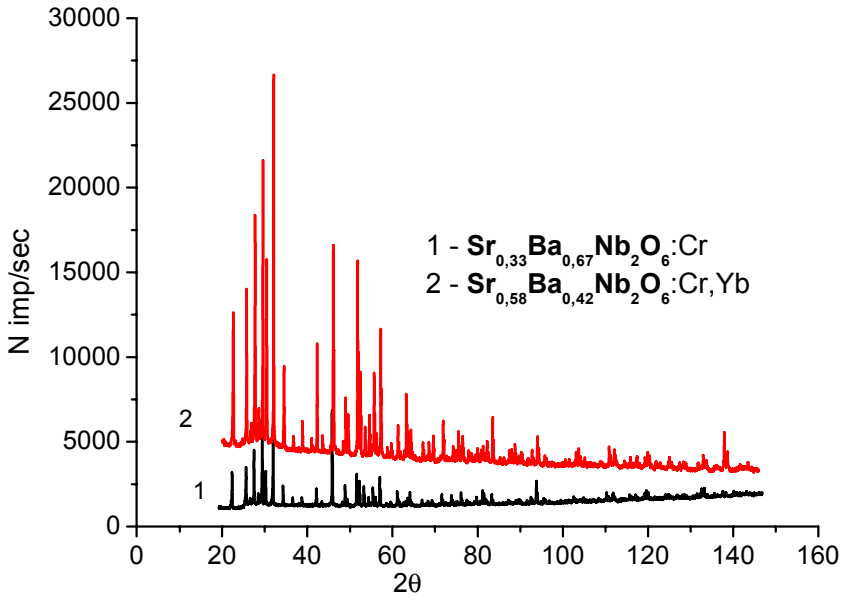

Fig. 1. XRD diffraction pattern of the investigated crystals.

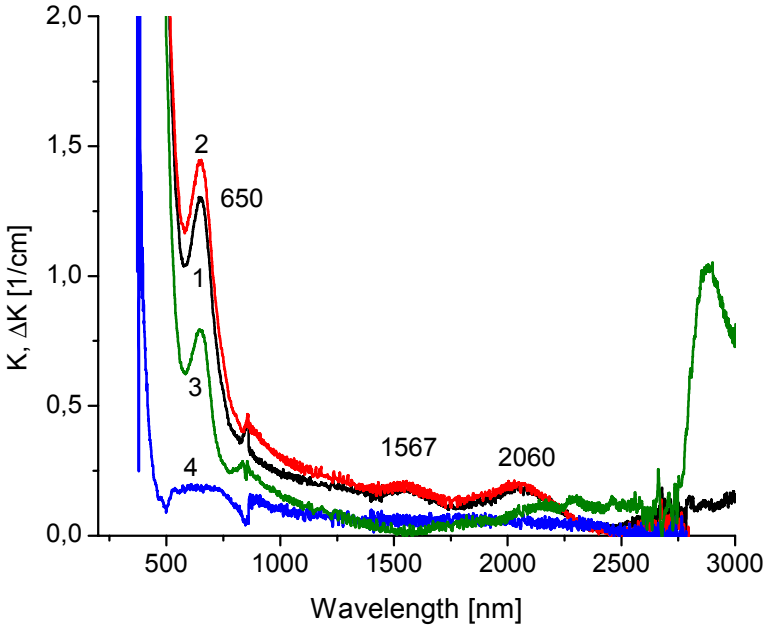

Fig. 2. The absorption spectra of as grown (1), γ-irradiated with a dose of $1.2 \cdot 10^5$ Gy (2) and additional absorption bands (4) of SBN:33:Cr, and, as grown (3) of SBN:58:Cr:Yb.

E500 EPR spectrometer with the field range 0÷1.4 T and the microwave field modulation of 100 kHz, in the Institute of Physics, Szczecin University of Technology. The magnetic field was scaled with a NMR magnetometer. Measurement was performed under the flow of helium gas, while the Oxford flow cryostat was employed to control the temperature. The rectangular sample cut out from bulk crystal for EPR purposes had dimensions 2.4 x 2.4 x 2.6 mm^3, where the largest size corresponded to the *c* crystal axis. The sample was glued to a quartz pipe and put into the resonance chamber.

In the frame of dielectrical measurements the hysteresis loops were recorded using modified Sawyer-Tower bridge and digital oscilloscope Tektronix. The field frequency was equal to 50 Hz. In the further study the following parameters: $\varepsilon'(T)$, $\varepsilon''(T)$ – real and imaginary components of the dielectrical permittivity, and, $\sigma(T)$ – conductivity, were measured. Dielectric loss was calculated as being equal to: $\mathrm{tg}(\delta(T)) = \varepsilon'(T)/\varepsilon''(T)$. Quantities of above parameters were examined as functions of field frequency in the range 1Hz-1MHz. The experimental setup for dielectric measurements contained the Hewlett Packard bridge HP4192A, temperature controller of Shimaden SR-30/Pt 100, sample chamber with nitrogen atmosphere and PC. Because we expected the diffused ferroelectric phase transition the graduation of temperature was chosen as high as 0.1K. All the measurements were made in Institute of Physics, Szczecin University of Technology.

3. RESULTS AND DISCUSSION

3.1. Optical spectroscopy

SBN belongs to a tungsten bronze family of ferroelectrics. In order to obtain the optical energy gap of SBN single crystals, we examined the following relation [8]:

$$(K^*h\nu)^2 = h\nu - E_g \qquad (2)$$

between the optical absorption coefficient *K* and the incident photon energy $h\nu$ valid for direct transitions between valence and conduction bands. The optical energy gap, E_g, obtained from (2) was found to be equal to 3.24 eV for pure SBN.

The absorption spectra of the SBN:33:Cr single crystals before and after γ-irradiation with a dose of 1.2^*10^5 Gy and SBN:58:Cr:Yb single crystals are

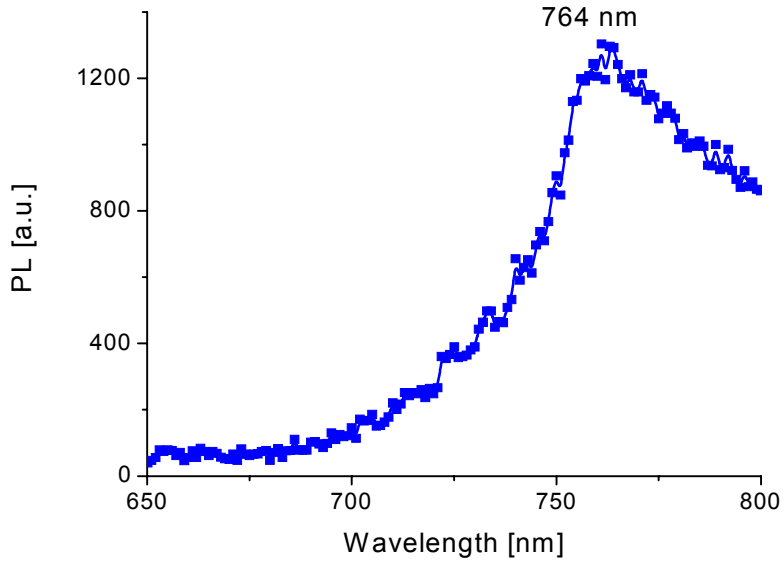

Fig. 3. PL band of SBN:Cr (0.02 wt.%) crystal underwent to γ-irradiation, λ_{ex}=488 nm.

presented in Fig. 2. For all crystals the fundamental absorption edge is equal to 370 nm while the IR lattice absorption starts at about 5400 nm. Both SBN:33:Cr and SBN:58:Cr:Yb crystals shown the broad absorption band around 650 nm (1.9 eV) and the strong absorption below 600 nm, very similar to the absorption bands of Cr^{3+} ions in other oxide crystals [9]. Two additional bands in the IR part of the absorption spectrum are observed, centered at 1567 and 2060 nm. The origin of these bands is unknown. In case of the SBN:58:Cr:Yb a strong absorption due to OH^- ions was observed at about 2863 nm. It indicates the necessity of the compensation of substituted ions. Irradiation with γ-quanta does not introduce distinct radiation defects so one can conclude that the crystal is radiation resistant.

A strong photoluminescence (PL) band in the NIR spectral band is observed in Cr and Cr, Yb doped SBN crystals. We have observed the 764 nm emission only when the crystals were underwent to γ-irradiation, what suggest that the Cr^{3+} ions substitute not only the Nb^{5+} ions but also are located at interstitials. In the earlier literature [10,11], pure SBN crystals are reported to exhibit a similar emission band in the same spectral range (around 760 nm). Our measurements confirm the existence of such emission band around 765 nm in nominally pure SBN crystals.

No *R*-line luminescence was observed in SBN:Cr and SBN:Cr, Yb crystals [11]. The PL band of the former crystal is presented in Fig. 3. In Fig. 4 excitation spectrum is shown.

Above 500 nm, the excitation spectrum resembles the absorption spectrum of the Cr^{3+} that means that the Cr^{3+} ions actually participate in the excitation process. The preliminary result shown [4,5] that the concentration of Nb in SBN:Cr decreases with increasing Cr concentration and the concentration of Sr/Ba does not depend of Cr, which means that the Cr^{3+} ions prefer to substitute for the Nb^{5+} ions. In the structure of SBN, Nb ions occupy B1 and B2 sites, which lie inside the distorted oxygen octahedra along the *c* axis of the crystal with slightly different Nb-O distances and different next nearest neighbor ions [7].

The substitution of the Cr^{3+} for the Nb^{5+} results in the splitting of the free Cr^{3+} ion states adequate for octahedral symmetry of crystal field. The 3d electron configuration of the Cr^{3+} is $3d^3$. The ground energy state of the free Cr^{3+} ions is ^4F and the excited states are ^4P, ^2G, ^2F and so on. Thus in octahedral crystal field, the Cr^{3+} states will split into ground state $^4A_{2g}$ and excited states ^2E_g, $^2T_{1g}$, $^2T_{2g}$, $^4T_{2g}$, $^4T_{1g}$, $^2A_{1g}$ and so on [6]. Surprisingly, there is only one broad absorption band at 650 nm resolved in SBN: Cr, as shown in Fig. 2. This broad band is similar to the $^4A_{2g} \rightarrow {}^4T_{2g}$ absorption band of the Cr^{3+}

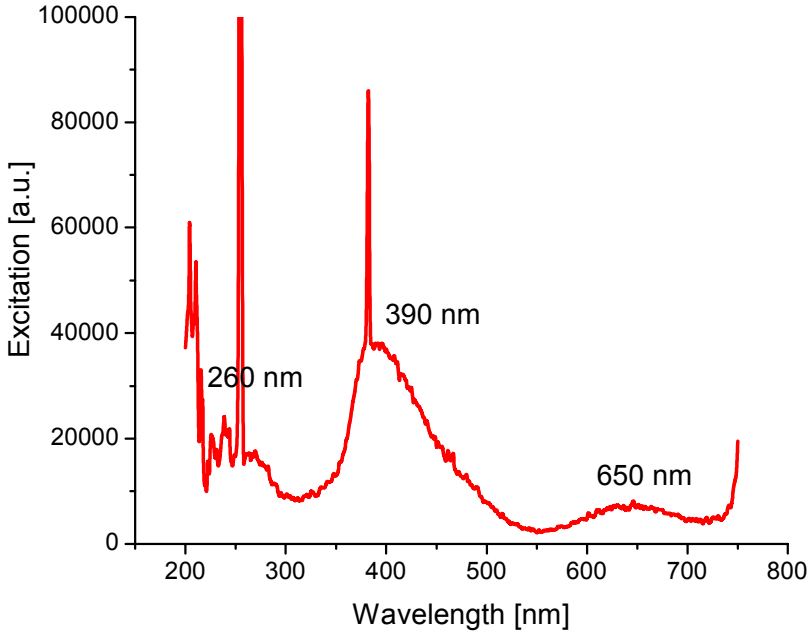

Fig. 4. Excitation spectrum of SBN: Cr (0.02 wt.%) crystal, λ_{em}=764 nm.

in emerald, $LiNbO_3:Cr^{3+}$ and $LiTaO_3:Cr^{3+}$ oxide crystals [7, 8], and therefore is assumed to origin from the same transition in the Cr^{3+} ion in octahedrally coordinated sites in SBN. The second broad absorption band due to the $^4A_{2g}\rightarrow{}^4T_{1g}$ transition cannot be resolved as separate band in SBN.

The absence of separated $^4A_{2g}\rightarrow{}^4T_{1g}$ transition band could be due to the fact that $^4T_{1g}$ state lies already inside the conduction band of SBN, and the $^4A_{2g}\rightarrow{}^4T_{1g}$ transition in the Cr^{3+} ion is dumped in the charge transfer $^4A_{2g}(Cr^{3+})\rightarrow 4d(Nb^{5+})$ transition.

In the case of SBN:58:Cr:Yb we expected that the Yb^{3+} substitutes the Nb^{5+} ions; but, unexpectedly, the substitution was not observed in both the absorption and PL spectra, although very high intensity of the 2863 nm band suggests presence of OH^- ions compensating such substitution (see Fig. 2, curve 3).

3.2. EPR measurements

Both samples: SBN:33:Cr and SBN:58:Cr:Yb have shown strong absorption of the magnetic field. We have observed EPR signal only in the case of SBN:33:Cr crystal and only for enough small sample. EPR absorption reveals single, intense, asymmetric, dysonian like line, centered at about *g*=2.1, while isolated chromium centers give usually EPR signal centered at about *g*~1.98. The temperature dependence of the EPR signal is presented in Fig. 5. The integrated intensity of the line reveals Curie behavior: decreases when temperature increases. The same concerns peak-to-peak linewidth. The EPR line vanishes at about 100K. *g*-factor does not depend of angle of crystal rotation in [010] and [001] planes and of temperature. It may indicate that the Cr^{3+} ions arise in the crystal mainly at interstitial positions.

3.3. Dielectric properties

As it is known from previous investigations [7], the transition from paraelectric to ferroelectric phase in case of $Sr_xBa_{1-x}Nb_2O_6$ crystal reveals a relaxor type behavior. For undoped SBN crystals (x=0.75) the transition temperature, T_C, was found to be equal to 348±5K [7]. This temperature generally depends on the crystal stoichiometry, type of doping, the procedure of temperature change (ascending or descending), and time factor.

In Fig. 6a one can see temperature dependencies of ε' in case of pure SBN (T_c=389K), and SBN:33:Cr for three subsequent experiments (T_c=386K, 382K, and 378K) performed for the same sample, for ascending temperature. As can be seen, the T_c decreases in subsequent experiments, moreover, the maximum of the ε' decreases ("fad-

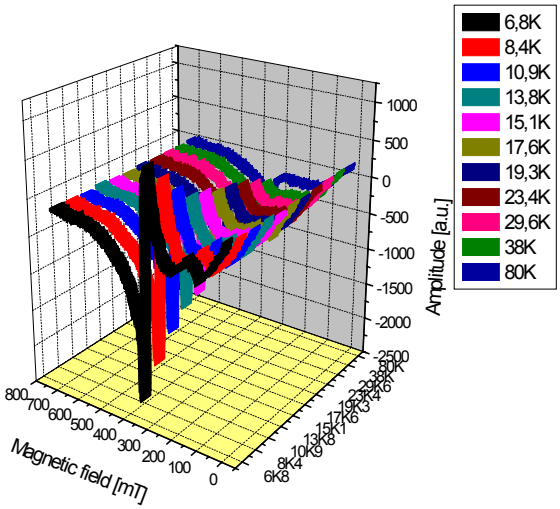

Fig. 5. EPR signal of the SBN:33:Cr single crystal versus temperature in the range 6-80K, *f*=9.44 GHz.

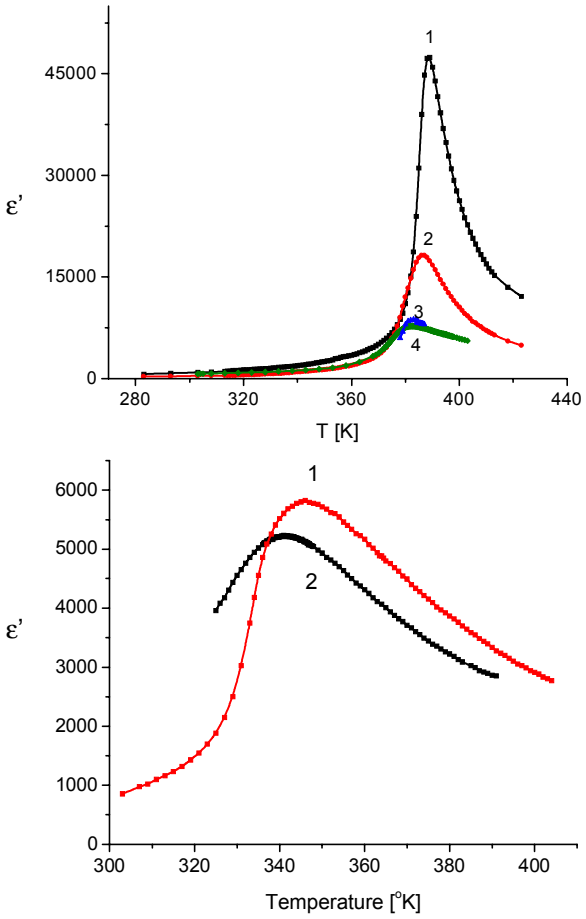

Fig. 6. Dielectric permittivity as a function of a temperature in ascending regime for: a): 1) SBN pure crystal (T_c=389K), 2) SBN:33:Cr (T_c=386K), 3) SBN:33:Cr after 2 weeks (T_c=382K), 4) SBN:33:Cr after 3 weeks (T_c=378K), b): 1) SBN:58:Cr:Yb for increasing temperature (T_c=346K), 2) SBN:58:Cr:Yb for decreasing temperature (T_c=340K); field frequency 1 kHz.

ing effect"). From Fig. 6b, where ascending and descending regimes of the temperature change were applied to SBN:58:Cr:Yb single crystal, it is seen that T_c is different in different regimes, and temperature dependence of the ε' is more broad in case of descending regime.

For the crystals obtained in Institute of Physics, Szczecin University of Technology, i.e. pure and chromium doped (0.02%) (*x*=0.33) (SBN:33:Cr), we registered the phase transitions (in descending regime) at temperature 382K and 378K, respectively. It indicates that Cr doping shifts slightly T_c value towards lower temperatures. For the crystal (x = 0.58) doped with chromium and ytterbium (SBN:58:Cr:Yb), we have found T_c = 340K (see Fig. 9) what is close to T_c=345K obtained for SBN:60:Cr [3] and T_c=348K obtained for SBN:75:Cr [7].

Considering Fig. 7, one can analyze the influence of quantity *x* and ytterbium codoping on phase transition parameters such as a shape and temperature. In the case of SBN:58:Cr:Yb, the maximum of the ε'(T) is lower and more broader then for SBN or SBN:33:Cr and is shifted towards lower temperature.

As it is known, the higher *x* results in higher T_c [12]. Decrease of T_c in the case of SBN:58:Cr:Yb could suggest the influence of Yb codoping. RE ions codoping reflects in the decreasing of T_c value [13]. However, it is known from [3] that SBN:60:Cr reveals T_c close to SBN:58:Cr:Yb. So, the change in value of T_c is not due to Yb codoping but due to

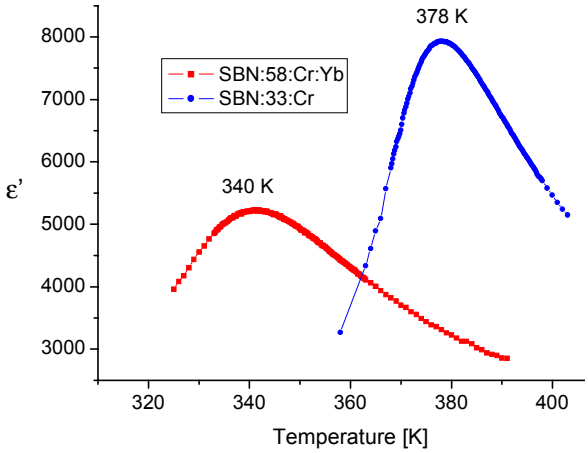

Fig. 7. The dependence of the ε'(T) registered for SBN:58:Cr:Yb and SBN:33:Cr crystals for field frequency 1 kHz.

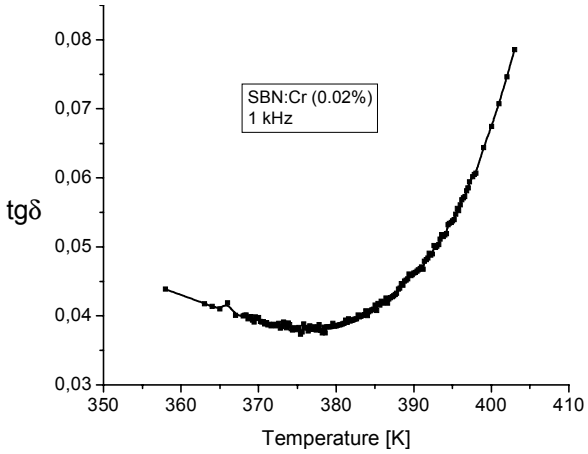

Fig. 8. The temperature dependence of loss tangent tgδ(*T*) for SBN:33:Cr crystal and the field frequency *f* =1 kHz.

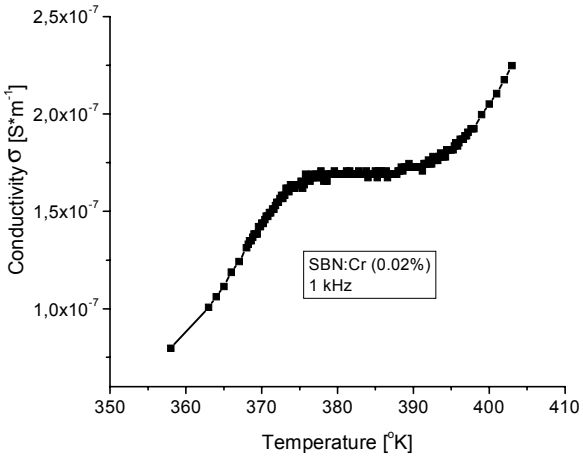

Fig. 9. The conductivity dependence σ(*T*) for the SBN:33:Cr crystal and the field frequency *f* = 1 kHz.

a change in crystal stoichiometry. This conclusion confirms the result that absorption does not show the Yb^{3+} related absorption.

As can be seen from Figs. 8 and 9, in the area of phase transition the loss tangent of SBN:33:Cr crystal achieves minimum while conductivity stay almost constant. The investigations of the conductivity versus electric field frequency have shown clear maximum at about 200 KHz.

Polarisation hysteresis loops are shown for SBN:33:Cr and SBN:58:Cr:Yb crystals in Fig. 10 and Fig. 11. The presented results were obtained for different values of AC field but for the same frequency, *f* = 50Hz. Using above results one can calculate a coercive field, E_c, and spontaneous polarization, *P* ($P(T)=P_o(1-T/T_c)^{\beta}$). Value of E_c is equal to about 48 kV/m for SBN:33:Cr and 50 kV/m for SBN:58:Cr:Yb and does not change with the amplitude of AC field.

The value of spontaneous polarization *P*, differs in both crystals and is equal to 2,44 μC/cm² and 1 mC/cm² for SBN:33:Cr and SBN:58:Cr:Yb, respectively. For comparison typical values of spontaneous polarization are: 20 mC/cm² for $BaTiO_3$ and 3 mC/cm² for TGS. We have observed that after a few times of measurement cycles in the temperature domain (heating/cooling) the shapes of the hysteresis loops were changed. It can be caused by electrical field in which the crystals were

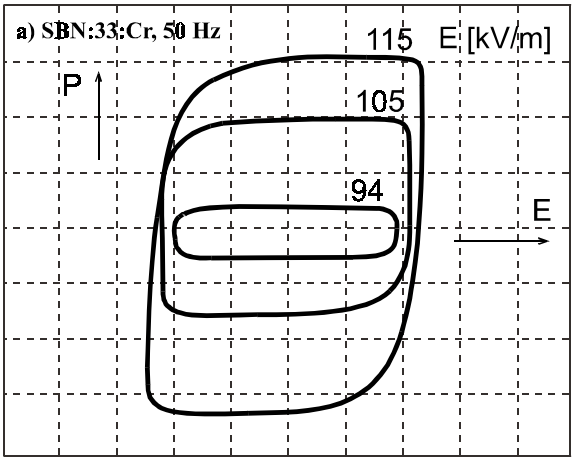

Fig. 10. The polarization hysteresis loop of SBN:33:Cr single crystal at three different amplitudes of an AC field at a frequency 50 Hz. Vertical scale is 2.44 μC/cm² per large div., horizontal scale is 48 kV/m per large div.

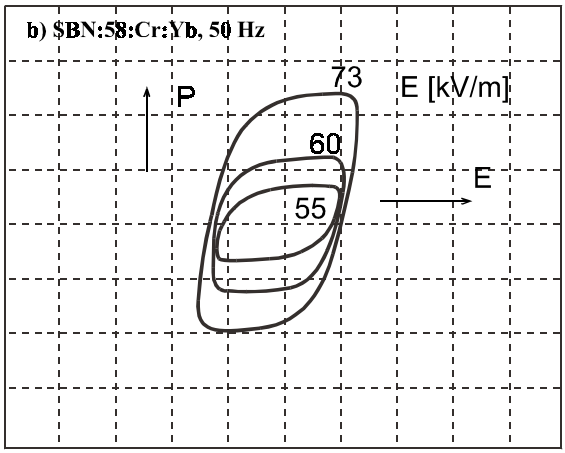

Fig. 11. The polarization hysteresis loop of SBN:58:Cr:Yb single crystal at three different amplitudes of an AC field at a frequency of 50 Hz. Vertical scale is 1.00 μC/cm² per large div., horizontal scale is 50 kV/m per large div.

examined and can be interpreted as “memory effect”.

4. CONCLUSIONS

The observed absorption and emission spectra of the investigated SBN:33:Cr and SBN:58:Cr:Yb single crystals are due to Cr^{3+} ions placed at octahedral Nb^{5+} positions and at interstitials. In case of SBN:Cr:Yb we observed strong OH^- absorption as an effect of the compensation of substituted ions. EPR results confirmed the presence of interstitial Cr^{3+} ions. Phase transition temperature from paraelectric to ferroelectric phase exhibits the dependence on the crystal stoichiometry, being equal to: T_c=382K, T_c=372K, T_c=340K, for pure SBN, SBN:33:Cr and SBN:58:Cr:Yb, respectively, type of doping (generally increase in RE and TM content lowers T_c value), and is a factor of time. Spontaneous polarization we have found being equal to P = 2,44 μC/cm^2 (SBN:33:Cr), and to P = 1 μC/cm^2 (SBN:58:Cr:Yb). The crystals exhibit also fading and memory effects.

ACKNOWLEDGEMENTS

Authors deeply acknowledge to Dr hab. Katarzyna Matyjasek from Institute of Physics, SUT, Poland, for hysteresis loops measurements. This work was partially supported by the grant No. 11-072-0120/17-88-00 (to S.M.K.)

REFERENCES

[1] T. Volk, L. Ivleva, P. Lykov, N. Polozkov, V. Salobutin R. Pankrath and M. Wohlecke // *Optical Materials* **18** (2001) 179.

[2] K. Buse // *Appl. Phys. B* **64** (1997) 273.

[3] K. Sayano, G.A. Rakuljic, A. Granat, A. Yariv and R.R. Neurgaonkar // *Optics Letters* **14** (1989) 459.

[4] R. Skulski, *Rozmycie przemian fazowych w wybranych grupach ferroelektryków i relaksorach* (Wydawnictwo Uniwersytetu Śląskiego, Katowice, 1989), In Polish.

[5] A.E. Andreichuk, L.M. Dorozhkin, Yu.S. Kuzminov, I.A. Maslyanitsin, V.N. Molchanov, A.A. Rusakov, V.I. Simonov, V.D. Shigorin and G.P. Shipulo // *Kristallografiya* **29** (1984) 1084, In Russian.

[6] PDF 39-0265: GRNT 1988, Scheetz, B., Nelson, Zellmer, Smith, Penn State University, University Park, PA, USA.

[7] P.B. Jameson, S.C. Abrahams and J.L. Bernstein // *The Journal of Chemical Phys*. **48** (1968) 5048.

[8] J. I. Pankove, *Optical Processes in Semiconductors* (Dorver, New York, 1971).

[9] D.L. Wood, J. Ferguson, K. Knox and J. F. Dillon Jr. // *J. Chem. Phys.* **39** (1963) 890.

[10] N. Giles, J. Wolford, G. Edwards and R. Uhrin // *J. Appl. Phys.* **77** (1995) 976.

[11] A. Zeinally, N. Lebedeva, A. Mordukhajev and M. Osman // *Ferroelectrics* **45** (1982) 83.

[12] R. Neurgaonkar, W. Hall, J. Oliver, W. Ho and W. Cory // *Ferroelectrics* **87** (1988) 167.

[13] P.L. Zhang, W.L. Zhong, Y.Y. Song and H.C. Chen // *Ferroelectrics* **142** (1993) 115.